Cell. Mol. Life Sci. 65 (2008) 1596 – 1608
1420-682X/08/101596-13
DOI 10.1007/s00018-008-8065-7

Cellular and Molecular Life Sciences

Research Article

Pharmacological manipulation of L-carnitine transport into L6 cells with stable overexpression of human OCTN2

L. Todesco[a, †], D. Bur[b, †], H. Brooks[a], M. Török[a], L. Landmann[c], B. Stieger[d] and S. Krähenbühl[a, *]

[a] Division of Clinical Pharmacology and Toxicology and Department of Research, University Hospital, 4031 Basel (Switzerland), Fax: +41-61-265-4560, e-mail: kraehenbuehl@uhbs.ch
[b] Actelion Ltd., Allschwil (Switzerland)
[c] Institute of Anatomy and Embryology, University of Basel, Basel (Switzerland)
[d] Division of Clinical Pharmacology and Toxicology, University Hospital Zurich, Zurich (Switzerland)

Received 5 February 2008; received after revision 14 March 2008; accepted 31 March 2008
Online First 14 April 2008

Abstract. The high-affinity Na^+-dependent carnitine transporter OCTN2 (SLC22A5) has a high renal expression and reabsorbs most filtered carnitine. To gain more insight into substrate specificity of OCTN2, we overexpressed hOCTN2 in L6 cells and characterized the structural requirements of substances acting as human OCTN2 (hOCTN2) inhibitors. A 1905-bp fragment containing the hOCTN2 complete coding sequence was introduced into the pWpiresGFP vector, and L6 cells were stably transduced using a lentiviral system. The transduced L6 cells revealed increased expression of hOCTN2 on the mRNA, protein and functional levels. Structural requirements for hOCTN2 inhibition were predicted *in silico* and investigated *in vitro*. Essential structural requirements for OCTN2 inhibition include a constantly positively charged nitrogen atom and a carboxyl, nitrile or ester group connected by a 2–4-atom linker. Our cell system is suitable for studying *in vitro* interactions with OCTN2, which can subsequently be investigated *in vivo*.

Keywords. hOCTN2, secondary carnitine deficiency, drug-carnitine interactions, stable transfection, acylcarnitines, verapamil.

Introduction

Carnitine is essential for the transport of activated long-chain fatty acids into the mitochondrial matrix of most cell types, where they can be metabolized by β-oxidation [1, 2]. Beside its role in the transport of long-chain fatty acids, carnitine also enables the removal of potentially toxic short acyl groups, *e.g.*, acetate or propionate, from the mitochondrial matrix and/or cytosol [3, 4].

Loss of carnitine from the body is minimized by the Na^+-dependent high-affinity carnitine transporter OCTN2, which is primarily responsible for reabsorption of filtered carnitine in the kidney [5–8]. The importance of this carnitine transporter becomes apparent from the severe consequences of OCTN2-related disorders. In primary systemic carnitine deficiency (CDSP, OMIM 212140) [1, 4–9], caused by mutations in the *SLC22A5* gene encoding for OCTN2, cellular (re)-uptake of carnitine is impaired [10–15]. Clinical findings in patients with primary carnitine deficiency result from low tissue carnitine levels and include myopathy, cardiomyopathy, hepatomegaly

† These authors contributed equally to this work.
* Corresponding author.

and failure to thrive [15–17]. Mutations in *SLC22A5* (OCTN2) found more recently were also associated with peripheral neuropathy [18] and ventricular fibrillation [19].

Besides the well-known roles of carnitine, several studies suggest that carnitine is involved in a multitude of other processes, for instance sperm quality assurance, immune responses or myocardial integrity and function, explaining the large interest for carnitine and OCTN2 [20–22].

Various drug interferences with carnitine transport [23–25] have been reported to cause secondary carnitine deficiency. Interference of various xenobiotics with OCTN2 has been characterized by Ohasi et al. [26]. Cephalosporin antibiotics comprising a quaternary nitrogen have been shown to inhibit OCTN2-mediated carnitine reabsorption in the kidney [27]. Structural features in these compounds mimicking physicochemical properties of carnitine may be responsible for inhibition of carnitine transport by OCTN2. Alternatively, allosteric interactions between xenobiotics and human OCTN2 (hOCTN2) may also be possible. Such drug-carnitine interactions may impair renal reabsorption of carnitine, possibly resulting in secondary carnitine deficiency.

In the present study, the transport characteristics of carnitine into different cell lines were determined to identify a suitable cell line for overexpressing hOCTN2. Subsequently, a stably transfected cell line was established, allowing the study of hOCTN2-driven carnitine transport. Some functional characteristics of this artificial hOCTN2 system were assessed and kinetic parameters of L-carnitine transport determined. Furthermore, this system enabled us to test the functionality of hOCTN2 in the presence of a variety of carnitine analogues as well as compounds comprising quaternary ammonium groups without structural similarity to carnitine and other compounds lacking structural similarities to carnitine.

Materials and methods

Reagents. All chemicals were purchased from Sigma, except L-carnitine, which was obtained from Fluka (Buchs, Switzerland). L-[^{3}H]carnitine hydrochloride (81 Ci/mmol) was obtained from Amersham-Pharmacia Biotech (Little Chalfont, Buckinghamshire, UK). Trimethylhydrazinium propionate was synthesized as described previously [28].

Cell culture. L6 cells (rat skeletal muscle myoblasts, obtained from American Type Culture Collection, Rockville, USA) and EBNA cells (human primary embryonal kidney, also from American Type Culture Collection) were grown in Dulbecco's modified Eagle's medium (DMEM), supplemented with 10 % fetal bovine serum (FBS), 1 mM sodium pyruvate and 100 U/ml penicillin and 100 µg/ml streptomycin (all substances from Invitrogen, Switzerland) at 37°C with 5 % CO_2 and 95 % humidity.

Preparation of polyclonal antibodies against OCTN2. The polyclonal antibody anti-OCTN2/K33 was generated to recognize a C-terminal amino acid sequence of the rat OCTN2 (amino acids 543–557). The peptide was coupled at the N terminus to keyhole limpet hemocyanin (KLH) to increase its immunogenicity. The structure of the construct was as follows: KLH-Tyr-Lys-Asp-Gly-Gly-Glu-Ser-Pro-Thr-Val-Leu-Lys-Ser-Thr-Ala-Phe-COOH. Rabbits were immunized and serum obtained as described previously [29].

Characterization of the antibodies. The antibodies were characterized by Western blotting of human and rat tissues, peptide competition and *in situ* hybridization in rat tissue. Male Sprague Dawley rats (150–200 g) housed under standard conditions were killed by decapitation, tissues were excised and immediately frozen in liquid nitrogen. Human tissues were obtained from cadavers <20 h post mortem (Institute of Pathology, University Hospital, Basel).

For Western blotting, tissues were homogenized at a concentration of 1 g/6 ml with a polytron homogenizer (Kinematica, Switzerland) in cold homogenization buffer [20 mM Tris-HCl pH 6.8, 1 % SDS, 1 mM DTT, containing Complete Mini® anti-protease cocktail (Roche, Switzerland)] and centrifuged (700 *g*, 5 min) at 4°C. Homogenate (50 µg protein) was combined with the same volume of loading buffer (2 % SDS, 10 % glycerol, 100 mM Tris-HCl pH 6.8, bromophenol blue, 5 mM DTT), heated to 50°C for 3 min and loaded onto a 10 % SDS-polyacrylamide gel. Proteins were separated in Tris-glycine running buffer (25 mM Tris, 192 mM glycine, 0.1 % SDS, pH 8.3) and transferred to nitrocellulose filters (Hybond ECL, APBiotech, Piscataway, USA) using a wet-transfer cell (Bio-Rad, Reinach, Switzerland) in a buffer containing 25 mM Tris, 192 mM glycine, pH 8.3, and 10 % methanol (1 h, 400 mA). The filter was blocked in 3 % defatted milk powder in PBS and exposed to the primary antibody anti-OCTN2/K33 antiserum (1:1000) in PBS/milk for 2 h. Secondary horseradish peroxidase-conjugated antibody to rabbit IgG (APBiotech) was used 1:5000 for 30–45 min in PBS/milk and the blot was rinsed four times in PBS/milk and twice in PBS. Antibody binding was visualized with an ECL detection system (APBiotech).

For peptide competition experiments, anti-OCTN2/K33 rabbit serum was preincubated with an excess of either the specific immunogen or a similar nonspecific peptide. Briefly, 2 µl rabbit sera (30 µg or 200 pmol IgG) was pre-adsorbed with 50 µg (30 nmol) of the nonspecific antigen K34/OCTN2 (KLH-Tyr-Leu-Pro-Asp-Thr-Ile-Asp-Gln-Met-Leu-Arg-Val-Lys-Gly-Ile-Lys-COOH) or specific antigen (K33/OCTN2) at room temperature in 500 µl PBS for 2 h. Two nitrocellulose filters were prepared containing electrophoresed samples (25–50 µg) of a rat kidney heavy and a rat kidney light membrane fraction (see below). After 2 h, the volume of the antigen-antibody solution was made up to 4 ml in PBS 3 % milk (1:2000 dilution of sera) and applied separately to one of the nitrocellulose filters. The filters were incubated for 2 h room temperature with either one of the pre-adsorbed antisera, washed and detection continued using a normal Western blotting procedure.

For the preparation of the membrane fractions, 1 g rat kidney was cut frozen (–70°C), minced with scissors and homogenized with a polytron in 6 ml ice-cold homogenization buffer (0.25 M sucrose, 10 mM Tris-HCl pH8, anti-protease cocktail Roche). The resulting homogenate was centrifuged at 800 *g* 4°C for 5 min and the supernatant centrifuged at 10 000 *g* 4°C for 15 min. The supernatant was then subjected to a 150 000 *g* spin for 1 h in a Beckman ultracentrifuge (SW55Ti rotor, Beckman, Nyon, Switzerland) and the resulting pellet was resuspended in 1 ml homogenization buffer containing 8 % (w/v) sucrose and loaded onto a sucrose gradient (20/30/40/50/70 % w/v sucrose in Tris buffer, pH 8). The gradient was spun for 18 h at 80 000 *g* in a swing out rotor (SW28 rotor, Beckman) and the visible protein fractions at the 40/50 % (fraction 4 = heavy fraction, k4) and at the 20/30 % interface (fraction 6 = light fraction, k6) were collected, diluted in Tris buffer pH 8 (no sucrose) and pelleted at 100 000 g for 1 h. The pellets were resuspended in 100–1000 µl homogenization buffer and the protein concentration assayed (Bio-Rad protein assay reagent using BSA as a standard). The heavy membrane fraction gave a strong signal with antibodies against Na^+/K^+ ATPase and aminopeptidase N, indicating a high brush border membrane content (data not shown). In the lighter membrane fraction, these signals were less pronounced (not shown).

For *in situ* hybridization experiments, rat and human tissues were freshly collected, cut into 2–3-mm cubes, and placed into 4 % paraformaldehyde in PBS for 3–16 h at 4°C with gentle shaking for fixation. Tissues were rinsed in multiple changes of PBS and stored in 25 % PVP-10 sucrose in PBS, 4°C overnight. Tissues were mounted on silane-coated slides and sections blocked prior to labeling with a 1:20 solution of goat serum in PBS/BSA blocking solution. Immunolabeling was performed at room temperature and antibodies diluted in wash solution (PBS + 0.5 % BSA). Primary antibody was anti-OCTN2/K33 1:200 and secondary antibody was Cy2-labeled goat anti-rabbit 1:300. Wash steps were for 15 min with four to five changes of buffer, primary antibody was allowed to bind for 1 h and the secondary for 30–45 min insulated from light. The labeled coverslips were mounted onto glass slides and allowed to set before visualizing. The slides were viewed using a Zeiss axiophot fluorescent microscope and images taken with analySIS software (Zeiss Instruments, Heerbrugg, Switzerland).

Production of lentiviral vectors and transduction of L6 cells. A 1905-bp fragment containing the hOCTN2 complete coding sequence was isolated from EBNA cells and introduced into the pWpiresGFP vector (kind gift of Dr. Didier Trono, University of Geneva). The new recombinant plasmid was verified on mutations by DNA sequencing. Lentiviral vector envelope plasmid pMD2.G and packaging plasmid pCMCΔR8.91 were kindly provided by Dr. Didier Trono. For the production of HIV-derived vectors, the envelope plasmid pMD2.G, the packaging plasmid pCMCΔR8.91 and the vector plasmid pwPhOCT-N2iresGFP (or empty vector pwPiresGFP) were introduced into 293T cells by calcium phosphate precipitation as described [30]. After 12 h the medium was replaced. The supernatant was harvested at 38 h post transfection, centrifuged at 2500 rpm, filtered through a 0.45-µM filter and stored at 4°C. Fresh medium was added to the cells and, after 24 h, the harvest procedure repeated. The viral stocks were pooled, aliquoted and stored at –70°C.

Expression of hOCTN2 in L6 cells. L6 cells, grown to about 50 % confluency in six-well plates, were incubated with virus supernatant prepared as detailed in the preceding section in the presence of Polybrene® (Aldrich, Buchs, Switzerland). Success of transduction was estimated with fluorescence-activated cell sorting (FACS) analysis. Enhanced green fluorescent protein (EGFP)-positive cells were enriched by FACS and cell culture was continued with this population.

Expression of hOCTN2 in the transduced L6 cells was determined with quantitative real-time PCR. Total RNA was isolated with RNeasy® (Qiagen, Basel, Switzerland) as described by the manufacturer. Superscript ™ II together with oligo(dT) and Random Hexamer primers (Gibco BRL, Basel, Switzerland) was used for reverse transcription of 2 µg total RNA. Quantification was performed on a ABI PRISM 7700 Sequence Detector (PE Biosystems, Rotkreuz, Swit-

zerland). Reporter probes hOCTN2 and GAPDH FAM/TAMRA were from Eurogentec (Seraing, Belgium); the hOCTN2 and GAPDH forward and reverse primers were from Microsynth (Balgach, Switzerland). PCR conditions were 95°C for 10 min, preceded by a 2-min step at 50°C, and 40 cycles 95°C for 10 s, 60°C for 60 s. The total reaction volume was 25 µl. For each cell type, a serial dilution of DNA was used (range: 6.25–50 ng) to investigate whether the C_T method could be used for calculation. GAPDH primers and probe were: forward primer 5'-GGTGAAGGTCGGAGTCAACG-3' and reverse primer: 5'-ACCATGTAGTTGAGGTCAATGAAGG-3' and the probe 5'-CGCCTGGTCACCAGGGCTGC-3'. The primers for the carnitine transporter hOCTN2 were designed to amplify a region that is highly conserved between human and rodent species. The forward primer was 5'-C(A or C)TATGTGTTGGCCTGGCTG-3', the reverse primer 5'-AACTTGCCCACCATCACCAG-3' and the probe 5'-CTCTTCCTGGGTGGCAGTGTCCTTCTCT-3'.

Flow cytometry analysis and immunohistochemistry of L6 cells overexpressing hOCTN2. For immunohistochemistry, cells were grown for 24 h at 37°C in an eight-chamber slide coated with poly-D-lysine. After washing, cells were visualized by phase-contrast microscopy and, after incubation with anti-OCTN2 (1:200, 30 min) and/or fluorescent-labeled Cy3 sheep anti-rabbit Ig (1:300, 20 min), by fluorescence microscopy (Olympus IX 50, Hamburg, Germany).

For flow cytometry, cells were rinsed with PBS and harvested with 10 mM EDTA. The detached cells were pelleted, resuspended in PBS supplemented with 2% FBS, and passed through a filter (40 µM) to obtain single cells. Cells were fixed with 2% paraformaldehyde for 20 min, washed and incubated with anti-OCTN2 antiserum anti-OCTN2/K33 (1/200 dilution) for 30 min. Cells were washed again before adding the fluorescent-labeled Cy3 sheep anti-rabbit Ig (Sigma) for 20 min. For analytical cell sorting, 2×10^4 cells were used on a FACSCalibur analyzer (Becton Dickinson, Allschwil, Switzerland).

Functional characterization of L6 cells overexpressing hOCTN2. The functionality of the hOCTN2 construct was evaluated by L-[^{3}H]carnitine transport measured at 30°C. Cells were grown to confluency on 12-well plates (Becton Dickinson), washed twice with prewarmed sodium uptake buffer (116 mM NaCl, 5.3 mM KCl, 0.8 mM $MgSO_4$, 26.2 mM $NaHCO_3$, 1 mM NaH_2PO_4 , 5.5 mM D-glucose, pH 7.4) and then incubated for 5 min in 2 ml of this buffer. The total uptake of L-[^{3}H]carnitine was determined by incubating the cells with 0.5 ml sodium uptake buffer containing 50 µM L-carnitine (5 µCi/0.5 ml) for 8 min at 30°C. The uptake was stopped by the addition of 2 ml ice-cold choline wash buffer (116 mM choline chloride, 5.3 mM KCl, 0.8 mM $MgSO_4$, 26.2 mM choline bicarbonate, 1 mM KH_2PO_4 , 5.5 mM D-glucose and 1 mM L-carnitine, pH 7.4). After washing the cells twice with 2 ml ice-cold choline uptake buffer, they were solubilized with 1 ml 1% SDS (w/v). After addition of 5 ml scintillation fluid (Ultima-gold^{TM}, Packard Bioscience, Zürich, Switzerland), the cell-associated radioactivity was counted.

For the sodium-independent L-carnitine uptake, the sodium uptake buffer was replaced by choline uptake buffer (does not contain L-carnitine, but is otherwise identical with the choline wash buffer). Otherwise the same procedure was applied.

The sodium-dependent L-carnitine uptake was obtained as the difference between total L-carnitine uptake (L-carnitine uptake determined in the presence of the sodium uptake buffer) and sodium-independent L-carnitine uptake.

In experiments dealing with inhibition of transport, cells were preincubated for 15 min with 0.1 and 1.0 mM (or 0.05 and 0.5 mM) inhibitor candidates before starting the uptake experiments executed as described above.

The protein concentration was determined using the BCA assay (Pierce, Rockford, IL, USA).

Search for compounds mimicking carnitine. At first, known substrates of OCTN2 that interfere with the transport of L-carnitine were analyzed to identify common structural features that might be responsible for this behavior. Superposition of an energy-minimized 3D structure of L-carnitine on a X-ray structure of cephaloridine revealed a good match of the positively charged tetramethylammonium group and the carboxylate group of L-carnitine with the charged pyridinium nitrogen and the carboxylate groups in the antibiotic, respectively (Fig. 1A). The 3D structure of cephaloridine was obtained from the Cambridge Structural Database (CSD) [31]. It was tempting to assume a functional role for both the negatively ionizable carboxylate and the constantly positively charged ammonium groups, and thereby identifying critical pharmacophores in the interaction of L-carnitine with OCTN2 (Fig. 1B).

Subsequently, the Merck index [32] was searched for compounds comprising such a pharmacophore pattern with more or fewer constraints for the distance between the negative and positive charges (linker of two to six saturated C-C bonds). Further compounds were identified in the "Index Nominum 2000" (http://www.micromedex.com/products/indexnominum/).

Selected substances were divided into four groups (Fig. 1C): (1) Molecules comprising an ammonium ion connected to a carboxylic acid with a three- to five-atom linker; (2) molecules comprising ammonium ions and derivatives thereof but not bearing a carboxylic acid group; (3) molecules comprising a positively charged nitrogen in a heteroaromate with or without a carboxylic acid group; and (4) cephalosporins or other compounds lacking a permanently positive charge (Fig. 1C).
Selected substances were then tested for their inhibitory effect on L-carnitine transport using L6 cells overexpressing hOCTN2. The transport activity of L-carnitine was determined as described before.

Possible interactions between cefalotin and L-carnitine. Possible interactions between cefalotin and L-carnitine were studied by assessing the effect of L-carnitine on the absorption spectrum of cefalotin and by assessing the effect of cefalotin on the L-carnitine concentration during the L-carnitine transport experiments.
For studying the effect of L-carnitine on the absorption spectrum of cefalotin, cefalotin was dissolved at two concentrations (100 and 1000 µmol/l, respectively) in sodium uptake buffer (116 mM NaCl, 5.3 mM KCl, 0.8 mM $MgSO_4$, 26.2 mM $NaHCO_3$, 1 mM NaH_2PO_4 , 5.5 mM D-glucose, pH 7.4) and the absorption spectrum was obtained between 190 and 600 nm. After the addition of 100 µmol/l L-carnitine, the same absorption spectrum was obtained and the spectra were compared.
To investigate a possible effect of cefalotin on the degradation of L-carnitine, L6 cells overexpressing hOCTN2 were incubated in sodium uptake buffer (see above) containing different cefalotin concentrations (0, 100 or 1000 µmol/l) at 30°C. After the addition of L-carnitine (25 or 50 µmol/l), L-carnitine transport was allowed to proceed for 8 min. After this time, the reactions were stopped by centrifugation of the suspensions (10 000 *g* at 5°C for 1 min). The concentrations of free and total acid soluble carnitine were measured in the supernatant as described by Brass and Hoppel [33].

Kinetic analysis and statistic. The kinetic parameters of L-carnitine transport into L6 cells transfected with hOCTN2 were calculated using the program sigmaplot version 10 (Scientific Solutions, www.scientific-solutions.ch). After subtraction of the values obtained in the presence of choline from those in the presence of sodium, data were fitted using nonlinear least squares regression analysis to:

$$v = \frac{V_{max} \times S}{K_m + S}$$

where v and S are the uptake rate and the concentration of L-carnitine, respectively, V_{max} is the maximal transport rate for L-carnitine and K_m the Michaelis-Menten constant.
For the determination of the IC_{50} value for verapamil, the data were fitted to:

$$\text{Activity} = \frac{\max - \min}{1 + (x/IC_{50})^{\text{Hillslope}}}$$

using sigmaplot version 10. Max is maximal activity (inhibitor concentration zero), min is the minimal activity, x is the concentration of the inhibitor, IC_{50} the concentration of the inhibitor at 50 % inhibition of the activity and Hillslope the slope of the curve. Data are presented as mean ± standard deviation.

Results

Production and characterization of antibodies against OCTN2. One of two rabbits immunized developed antibodies against a protein of 67 kDa on the Western blot of rat kidney and rat kidney brush border membrane vesicles (data not shown). Further characterization of the antiserum (anti-OCTN2/K33) obtained from this rabbit showed that it also reacted with human kidney tissue (on Western blots) obtained post mortem (data not shown).
To demonstrate the specificity of the anti-OCTN2/K33 serum, a competition experiment with the peptide used for immunization was performed. As shown in Figure 2A (panel a), K33 pre-treated with an unspecific peptide identifies a 67-kDa protein in the k4 fraction of rat kidney. This band (indicated by an arrow) can also be detected in the k6 fraction, but is much fainter. After pre-treatment of anti-OCTN2/K33 with the peptide used for antibody production, both bands at 67 kDa vanished (Fig. 2A, panel b). Finally, as shown in Figure 2B, immunohistochemistry of rat kidney sections showed the expected localization of OCTN2 on the luminal side of proximal tubules. Similar results were obtained with human kidney (results not shown).

Characterization of hOCTN2 expression in stably transduced L6 cells. FACS analysis revealed a primary success rate of transduction of approximately 60 % in L6 cells. Cells were cultured and characterized first by mRNA expression of hOCTN2 using RT-PCR. Quantitative real time PCR showed a >250-fold increase of hOCTN2 mRNA expression in L6 transfected cells as

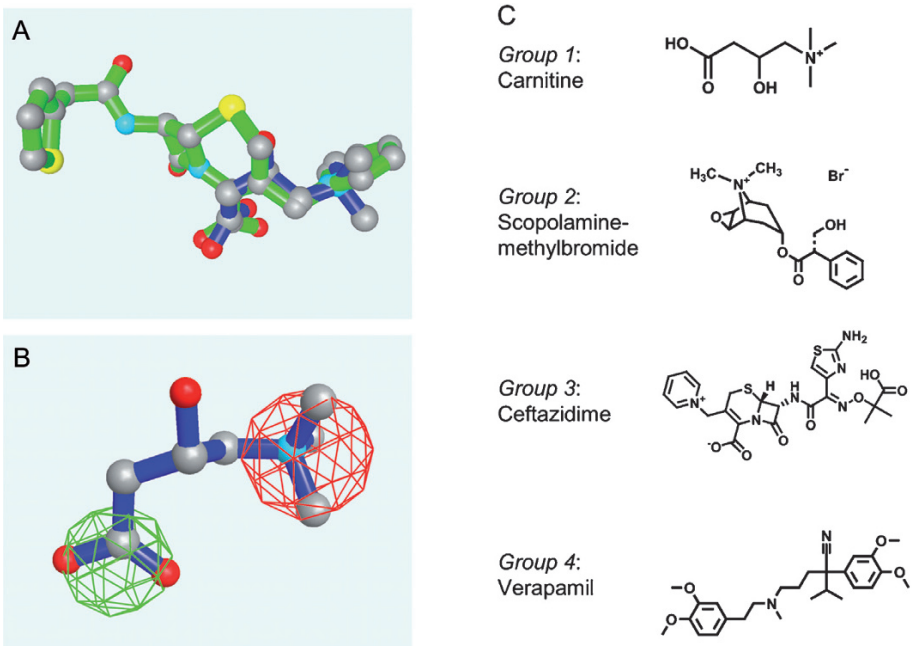

Figure 1. Characterization of the substances used as potential inhibitors of hOCTN2. (*A*) Superposition of L-carnitine (blue) on cephaloridine (green), showing the structural similarity. (*B*) L-carnitine (blue) with the two pharmacophores postulated: the ammonium functionality (red ball) and the carboxyl group (green ball). (*C*) The substances selected based structural similarity with L-carnitine and tested for inhibition of L-carnitine transport were (1) substances containing an ammonium ion connected to a carboxylic acid with a three- to five-atom linker, (2) ammonium ions and derivatives thereof not linked to a carboxylic acid group, (3) substances comprising a positively charged nitrogen in a heteroaromate with or without a carboxylic acid group, and (4) substances lacking a constantly positive charge (*e.g.*, cephalosporins, verapamil). Typical representatives of each group are shown.

compared to mock transfected L6 cells (not shown). The presence of the hOCTN2 transporter was further demonstrated by immunohistochemistry (Fig. 3A) and by FACS analysis (Fig. 3B).

The functionality of the hOCTN2 construct in L6 cells was evaluated by L-[^{3}H]carnitine uptake experiments, where, for assessing the sodium-independent uptake, Na^+ was replaced by choline in the transport buffer. We found the Na^+-dependent L-[^{3}H]carnitine uptake to be approximately 25-fold higher in hOCTN2 transduced L6 cells as compared to mock transfected L6 cells after 8 min of exposure at 30°C (Fig. 4A). In contrast, the Na^+-independent transport activity remained unchanged in transduced L6 cells as compared to the mock-transfected L6 cells. The uptake was linear for at least 8 min.

Next, the concentration dependency of the L-carnitine transport was determined and kinetic parameters were calculated. As shown in Figure 4B, the transport of L-carnitine was saturable after correction for a non-saturable component. The calculated K_m and V_{max} values for L-[^{3}H]carnitine transport are 9.7±0.3 μM and 290±4 pmol/mg protein/min, respectively.

Inhibitors of carnitine transport by hOCTN2. Four groups of compounds were selected as described in Material and methods, and subsequently tested for their capacity to interfere with L-carnitine transport by hOCTN2. Derivatives of L-carnitine and close structural analogs (group 1, *e.g.*, acylcarnitines, butyrobetaine and trimethylhydrazinium propionate) demonstrated a strong inhibition of the L-carnitine uptake by transfected L6 cells (Table 1). The nature of the atoms linking the charged group is not of critical importance for recognition by hOCTN2 (compare L-carnitine vs trimethylhydrazinium propionate). However, a linker length of at least three atoms between ammonium ion and carboxylate is crucial for recognition by the transporter, as is clearly indicated by the lack of interaction for betaine that comprises only a short linker. Substituents of different length connected to the linker are tolerated by hOCTN2 without loss of inhibition, unless the substituent is branched (Table 1, compare hexanoylcarnitine vs valproylcarnitine, pivaloylcarnitine). Interestingly, removal of a single methyl group and thereby the constant charge from the ammonium functionality results in complete loss of inhibitory power (Table 1, compare butyrobetaine vs dimethylaminobutyric acid). Replacement of the negatively charged carboxylate by an ester or inverted ester group did not decrease the inhibitory activity, as long as the linker consisted of at least three atoms (Table 2, *e.g.*, atropine methyl bromide, anisotropine methyl bromide, ipratropium bromide). Ap-

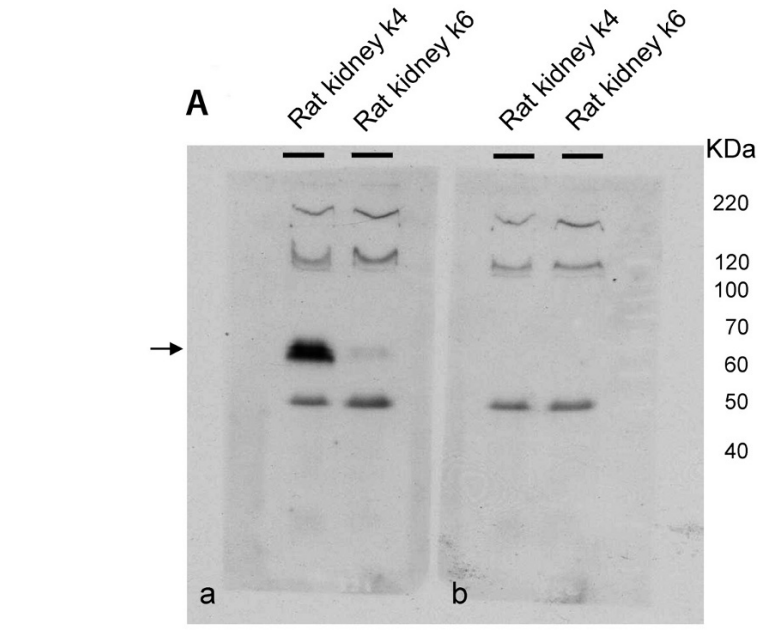

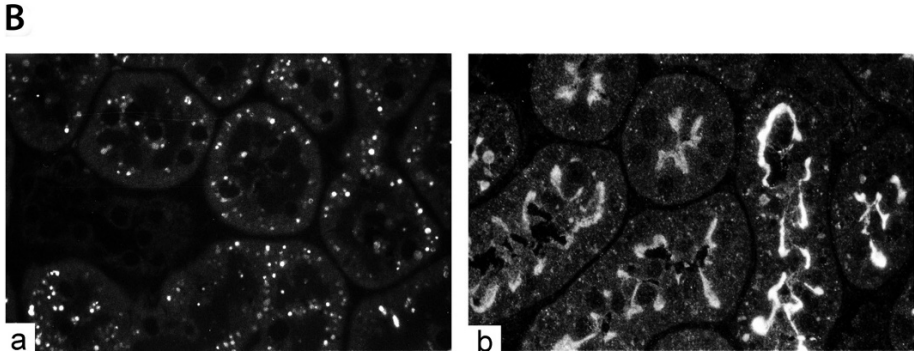

Figure 2. Characterization of the antiserum against a polypeptide of the preterminal region of rat OCTN2 (anti-OCTN2/K33). (*A*) Anti-OCTN2 serum treated with an unspecific peptide identifies a 67-kDa protein in the k4 (heavy membrane fraction) and, fainter, in the k6 fraction (light membrane fraction) of rat kidney (panel a). After pre-treatment of anti-OCTN2 serum with the peptide used for antibody production, both bands at 67 kDa have vanished (panel b). (*B*) Immunohistochemistry of rat kidney sections shows the expected localization of OCTN2 on the luminal side of proximal tubular cells in sections treated with anti-OCTN2 serum (primary antibody) and Cy2-labeled goat anti-rabbit (secondary antibody) (panel b). In sections treated with secondary antibody only, the fluorescence pattern is unspecific (panel a).

parently, the inactive scopolamine butyl bromide seems to disobey this rule; however, this lack of interaction with hOCTN2 may be a consequence of the extended alkyl group attached to the ammonium ion (Table 2, compare scopolamine methyl bromide vs scopolamine butyl bromide). Neostigmin bromide showed no inhibitory activity, either due to the exchange of the ester to a carbamate group or due to its very rigid geometry that could prevent productive interaction with the protein. Shortening the distance between ammonium ion and inverted ester or removing the ester function resulted in loss of the inhibitory activity (Table 2, see acetylcholine, carbamylcholine, decamethonium bromide).

Incorporation of the positive charge into a heteroaromate resulted in a substantial or complete loss of the inhibitory activity (Table 3). Interestingly, of the two cephalosporins comprising a constant positive charge only cefozopran showed a weak inhibitory activity, while ceftazidime did not interfere with L-carnitine transport at all, despite the presence of a three-atom linker between the charged pyridinium nitrogen and carboxylate. Pancuronium bromide displayed an unexpected weak inhibitory activity, despite comprising only a short two-atom linker between ammonium ion and inverted ester. Not surprisingly, pyridostigmine bromide comprising only a short linker as well as amprolium hydrochloride and hexadecylpyridinium bromide, which both lack the carboxylic acid functionality, were completely inactive.

All substances lacking the constantly ionized nitrogen were completely inactive up to this point (see Table 4 and dimethylaminobutyric acid in Table 1). One substance not following this rule was cefalotin, which appeared to stimulate transport of L-carnitine by OCTN2. To study the possible formation of a complex between cefalotin and L-carnitine, the absorption spectrum of cefalotin (100 or 1000 μmol/l) was obtained in the absence and presence of 100 μmol/l L-carnitine. Since the addition of L-carnitine did not change the absorption spectrum of cefalotin (data not shown), the formation of a complex between the two compounds

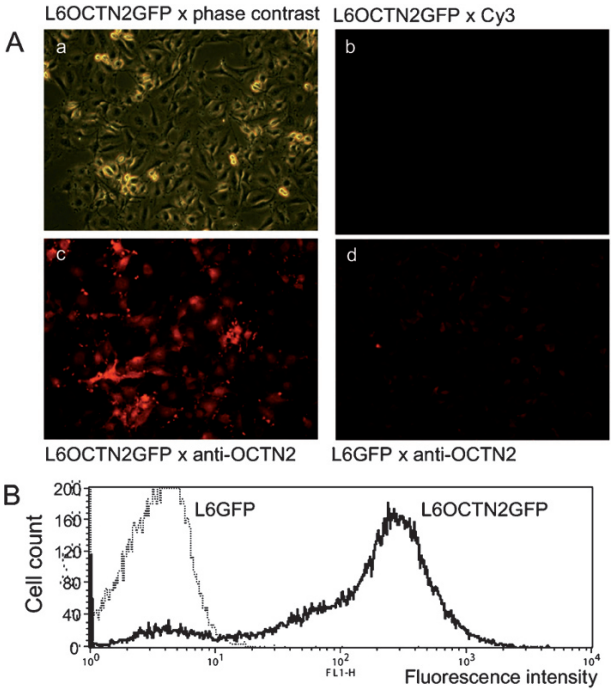

Figure 3. Morphological characterization of the L6 cells transfected with hOCTN2. (*A*) Cells were grown in an eight-chamber slide, washed and visualized by phase contrast microscopy (panel a). Other slides were incubated with anti-OCTN2 (1:200, 30 min) and/or fluorescent-labeled Cy3 sheep anti-rabbit Ig (1:300, 20 min) and assessed by fluorescence microscopy (panels b–d). A positive result by fluorescence microscopy is seen only in L6OCTN2GFP cells treated with the combination anti-OCTN2 and Cy3 sheep anti-rabbit Ig (panel c). (*B*) Cells were detached with 10 mM EDTA, fixed with 2 % paraformaldehyde for 20 min, washed and incubated first with anti-OCTN2 antiserum (anti-OCTN2/K33, 1:200 dilution) and then with Cy3-labeled sheep anti-rabbit Ig. For analytical cell sorting, 2×10^4 cells were used on a FACSCalibur analyzer. There is a clear shift of the signal in L6OCTN2GFP cells compared to L6GFP cells.

could be excluded under the conditions used. Furthermore, a possible inhibition of L-carnitine degradation by cefalotin was studied in incubations containing different L-carnitine (25 or 50 μmol/l) and cefalotin concentrations (0, 100, 1000 μmol/l). The results showed that L-carnitine is not degraded under the conditions studied and that cefalotin has no effect on L-carnitine degradation (data not shown), excluding this possibility as a reason for the observed increase in carnitine transport in the presence of cefalotin.

Another molecule behaving against the rule that a positive charge is required for interference with L-carnitine transport by OCTN2 was verapamil. In agreement with a previous report [34], verapamil hydrochloride was found to be a strong inhibitor of hOCTN2 (Fig. 1C). To further characterize this inhibitory effect exerted by verapamil, the IC_{50} was determined to be 5.3 μM (Fig. 5). In this context, the complete lack of inhibitory activity of dimethylaminobutyric acid is remarkable, considering its close topological relationship with the highly active butyrobetaine. In general, a permanent positive charge appears to be crucial for a compound interfering with L-carnitine transport by hOCTN2.

Discussion

The membrane protein OCTN2 is a member of the sodium-dependent organic cation transporters, with a high affinity for L-carnitine. In humans, OCTN2 is expressed strongly in kidney but only weakly in skeletal muscle, liver, lung, brain and small intestine [6], whereas the rat counterpart is highly expressed in

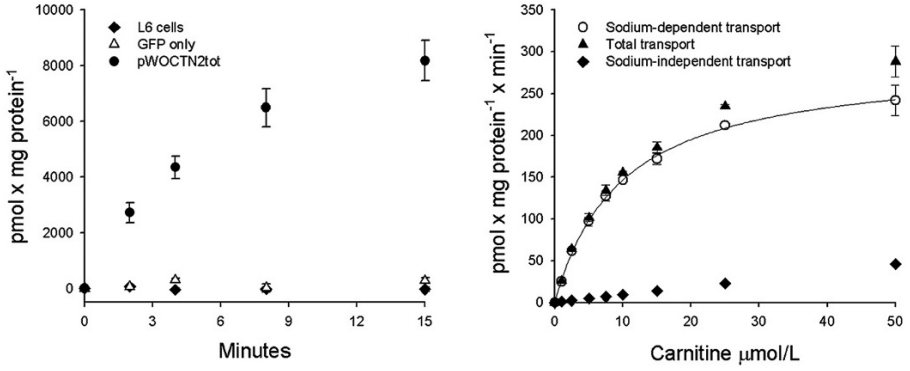

Figure 4. Functional characterization of the L6 cells overexpressing hOCTN2. The functionality of hOCTN2 was determined by L-[^{3}H]carnitine uptake experiments as described in Methods. (*A*) Time dependency of sodium-dependent L-carnitine transport. While no sodium-dependent transport of L-carnitine can be detected in non-transfected L6 cells or L6 cells transfected with GFP, L6 cells transfected with hOCTN2/GFP have a high sodium-dependent transport activity, which is linear up to at least 8 min. (*B*) Assessment of the kinetics of L-carnitine transport into L6OCTN2GFP cells revealed saturable sodium-dependent transport of L-carnitine after correction for the sodium-independent component. The calculated K_m and V_{max} values for L-[^{3}H]carnitine transport are 9.7±0.3 μM and 290±4 pmol/mg protein/min, respectively.

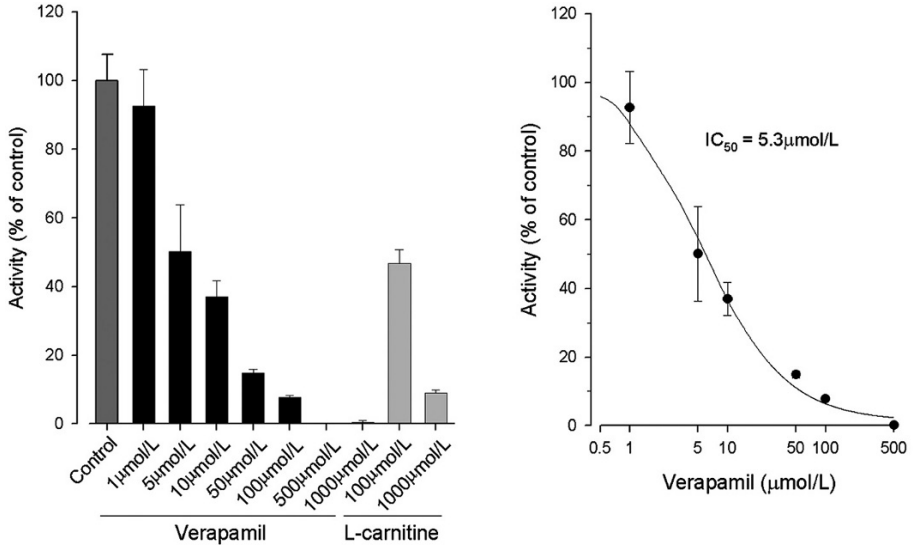

Figure 5. Inhibition of hOCTN2-driven transport of L-carnitine by verapamil. To investigate the interaction between hOCTN2 and verapamil in more detail, L-carnitine transport by L6 cells overexpressing hOCTN2 was studied at several verapamil concentrations (*A*) and the IC_{50} was determined (*B*). L-carnitine transport was determined as described in Methods and incubations containing excess L-carnitine were used as controls. Verapamil turned out to be a potent inhibitor L-carnitine transport with an IC_{50} of 5.3 µmol/l.

Table 1. Inhibition of hOCTN2 by substances carrying an ammonium ion and a carboxylic acid group. Inhibition was scored as follows: -, >80 % hOCTN2 activity in the presence of 100 or 1000 µM potential inhibitor; +, <80 % and >50 % hOCTN2 activity in the presence of 1000 µM inhibitor; ++, <50 % hOCTN2 activity in the presence of 1000 µM inhibitor; +++, <50 % hOCTN2 activity in the presence of 100 µM inhibitor.

Substance	Carnitine transport (% of control, inhibitor 100 µM)	Carnitine transport (% of control, inhibitor 1000 µM)	No. of atoms between pharmacophores	Efficacy of inhibitor
L-carnitine	49±4	15	3	+++
Acetylcarnitine	78±2	23±1	3	++
Pivaloylcarnitine	91±1	56±4	3	+
Hexanoylcarnitine	59±1	13±0	3	++
Octanoylcarnitine	63±3	18±1	3	++
Valproylcarnitine	96±8	77±3	3	+
Palmitoylcarnitine	80±5	20±?	3	++
Trimethylhydrazonium propionate	92±0	34±2	3	++
Butyrobetaine	57±3	16±1	3	++
Dimethylaminobutyric acid	102±1	94±2	3	–
Betaine	112±1	106±4	1	–

kidney and testis, but to a lesser extent in liver and small intestine [28, 35].

The substrate specificity of OCTN2 is broad, as several other cations, in particular carnitine derivatives and carnitine analogues are able to compete with and inhibit L-carnitine transport [7]. We therefore established and characterized a heterologous expression system designed for measuring transport inhibition of L-carnitine by compounds with more or less structural similarity. The strong inhibition exhibited by some of these selected compounds (Table 1) is consistent with reports found in the literature [7, 26, 36, 37]. Surprisingly, also therapeutics interfere with OCTN2-mediated L-carnitine transport [34], among them some members of the cephalosporin family as reported by Ganapathy et al. [27].

The interaction of certain cephalosporins with the OCTN2 transporter can most likely be attributed to the presence of a pharmacophore pattern (Fig. 1B) in the substances that mimic L-carnitine. As a working hypothesis, we assumed the pharmacophore pattern to consist of a quaternary nitrogen that is separated by three atoms from a carboxylic acid functionality, thereby mimicking the topology of L-carnitine. To test this hypothesis and to explore its rigidity, we selected compounds and divided them into four categories of as described in the results section.

Carnitine and close derivatives thereof (Table 1) have all a very profound inhibiting effect on L-carnitine

Table 2. Inhibition of hOCTN2 by substances carrying an ammonium ion and a carboxylic acid group or a derivative thereof. Substances were selected and tested for hOCTN2 inhibition as described in Methods. Inhibition was scored as described in Table 1.

Substance	Carnitine transport (% of control, inhibitor 100 μM)	Carnitine transport (% of control, inhibitor 1000 μM)	Functional group closest to ammonium nitrogen (distance in atoms)	Efficacy of inhibitor
Atropine methyl bromide	67±4	24±4	Inverted ester (3)	++
Anisotropine methyl bromide	93±11	47±9	Inverted ester (3)	++
Ipratropium bromide	38±2	29±2	Inverted ester (3)	++
Scopolamine methyl bromide	75±112	20±3	Inverted ester (3)	++
Scopolamine N-butyl bromide	103±6	102±5	Inverted ester (3)	–
Pancuronium bromide	93±2	59±2	Inverted ester (2)	+
Acetylcholine	85±5	83±3	Inverted ester (2)	–
Carbamylcholine chloride	102±1	94±2	Inverted ester (2)	–
Decamethonium bromide	88±3	91±9	None	–
Neostigmine bromide	91±4	85±11	Carbamate (3)	–

transport by hOCTN2. A linker of three atoms between the two functionalities (ammonium ion, carboxylic acid) appears to be critical as exemplified by the short-linked betaine being completely inactive. Substitutions at the linker are neither required nor forbidden and therefore without importance, as evidenced for butyrobetaine and trimethylhydrazinium propionate. Even long substituents such as palmitoyl are well tolerated as long as they are unbranched. The slightly decreased inhibitory activities of the branched linker substituents contained in valproyl- and pivaloylcarnitine (Table 1) might indicate a spatial restriction executed by hOCTN2 in the linker region.

The ammonium ion is crucial for recognition as can be seen from the complete inactivity of dimethylaminobutyric acid. To further evaluate the individual requirements of the two linked functional groups, a second set of compounds, either comprising a derivatized neutral carboxylic acid functionality or no such functionality, was selected (Table 2). If the ammonium functionality comprises at least two methyl substituents, an inverted ester separated by two atoms is well tolerated and even a branched isopropyl substituent (ipratropium bromide) or a bridge between two substituents (pancuronium bromide) of the charged nitrogen is still accepted by hOCTN2. Surprisingly, in scopolamine derivatives, there is a striking difference between the very well-recognized *N*-methyl compound and the more voluminous, but almost inactive, *N*-butyl derivative. A search through the PDB database [38] revealed a high preference for electron-rich aromatic side chains like tyrosine or tryptophan enclosing an ammonium functionality. Lengthy and more voluminous substituents like the *N*-butyl group might adversely interfere with a close contact between amino acid side chains and the ammonium functionality, and therefore hamper the recognition of scopolamine *N*-butyl bromide. A shortened two-atom linker between the ammonium functionality and an inverted ester is not tolerated in rather small molecules (Table 2, acetyl choline) and likewise introduction of a carbamate functionality is absolutely detrimental for recognition by hOCTN2 (Table 2, carbamylcholine, neostigmine). Absence of a carboxylic acid functionality also leads to non-recognition by the transporter (Table 2, decamethonium bromide).

A constant positive charge can reside not only in an ammonium ion but also in a heteroaromate as, for example, in cephaloridine that has been shown to interfere with L-carnitine transport by hOCTN2 [27]. To further assess the capability of hOCTN2 to transport various positively charged heteroaromates, we selected compounds comprising such an entity but lacking further constantly positive charged functionalities (group 3). The two charged cephalosporin derivatives showed either no (Table 3, ceftazidime) or only borderline activity (cefozoprane), despite the presence of a charged carboxylate group separated by a three-atom linker (ceftazidime). Of the other selected examples (Table 3), none showed significant activity, which could indicate a steric

Table 3. Inhibition of hOCTN2 by substances carrying a constant positive charge on a nitrogen in an aromate. Substances were selected and tested for hOCTN2 inhibition as described in Methods. Inhibition was scored as described in Table 1.

Substance	Carnitine Transport (% of control, inhibitor 100 μM)	Carnitine transport (% of control, inhibitor 1000 μM)	Functional group closest to positively charged nitrogen (no. of atoms between pharmacophores)	Efficacy of inhibitor
Ceftazidime	81±3	89±7	Carboxylate(3)	–
Cefozoprane	94±9	78±2	Carboxylate (5)	+
Amprolium hydrochloride	82±5	83±1	Amine (3)	–
Hexadecylpyridinium bromide	72±8	n.a.[1]	None	n.a.
Pyridostigmine bromide	92±6	92±4	Ester (2)	–

n.a.: not assessable.

handicap of the disc-shaped heteroaromates that cannot be properly recognized by the "active site" in hOCTN2.

Since cephaloridine is a known inhibitor of L-carnitine transport by hOCTN2 [27], it was more than tempting to check whether the cephalosporin scaffold *per se* without bearing a constant charge is recognized by the transporter. This question can be clearly negated since none of the eight tested cephalosporin or penicillin derivatives showed significant interference with the L-carnitine transport (Table 4). After exclusion of direct interactions between cefalotin and carnitine, the most likely reason for the observed stimulation of carnitine transport by cefalotin is an allosteric interaction with OCTN2, an assumption needing more detailed studies to be proven. So far, no other compounds with such properties have been described.

Table 4. Inhibition of hOCTN2 by substances comprising either a cephalosporin or penicillin scaffold and the structural outlier verapamil. Substances were selected and tested for hOCTN2 inhibition as described in Methods. Inhibition was scored as described in Table 1.

Substance	Carnitine transport (% of control, inhibitor 100 μM)	Carnitine transport (% of control, inhibitor 1000 μM)	Efficacy of inhibitor
Cefalotin	110±5	122±2	–
Cefoxitin	80±22	87±3	–
Ceftriaxone	84±9	83±5	–
Cefazolin	100±7	91±11	–
Cefamandole	90±6	96±2	–
Cefuroxime	97±8	84±5	–
Cephaloxin	91±8	82±13	–
Ampicillin	82±6	90±2	–
Verapamil	54±1	28±1	++

Not obeying the rules mentioned so far, verapamil (Fig. 1C) was identified as a strong inhibitor of hOCTN2 (Table 4 and Fig. 5). This molecule comprises neither a constantly charged nitrogen ion nor a carboxylic acid derivative separated by a three-atom linker. The inhibitory effect of verapamil on carnitine transport has been described in an oocyte system with hOCTN2 expression [34] and in heart and skeletal muscle explants [39], but the mechanisms of inhibition are so far not clear. It cannot be completely excluded that the tertiary nitrogen, in combination with the nitrile group, could be mimicking a pair of pharmacophores that are strongly recognized by hOCTN2. Alternatively, verapamil might be acting *via* an allosteric inhibitor and thereby not directly interfere with L-carnitine recognition and transport by hOCTN2.

Further studies are therefore necessary to understand the relationship between structure and inhibitory or stimulatory capacity of drugs and chemicals towards hOCTN2. Since inhibition of hOCTN2 by chemical compounds can be associated with systemic carnitine deficiency [27, 34], identification of hOCTN2 inhibitors appears to be clinically important. Our model provides the basis for identification and rapid screening of possibly interacting substances, but the clinical relevance of hOCTN2 inhibition observed *in vitro* needs to be studied in animals or humans *in vivo*. It has also to be taken into account that inhibition of hOCTN2 is not the only mechanism associated with secondary carnitine deficiency [26, 34].

Acknowledgements. The study was supported by a grant from the Swiss National Science Foundation to S.K. (310000–112483).

1 Bremer, J. (1983) Carnitine – Metabolism and functions. Physiol. Rev. 63, 1420–1480.
2 Fritz, I. B. (1955) The effects of muscle extracts on the oxidation of palmitic acid by liver slices and homogenates. Acta Physiol. Scand. 34, 367–385.

3 Bremer, J. (1990) The role of carnitine in intracellular metabolism. J. Clin. Chem. Clin. Biochem. 28, 297–301.
4 Treem, W. R., Stanley, C. A., Finegold, D. N., Hale, D. E. and Coates, P. M. (1988) Primary carnitine deficiency due to a failure of carnitine transport in kidney, muscle, and fibroblasts. N. Engl. J. Med. 319, 1331–1336.
5 Tamai, I., China, K., Sai, Y., Kobayashi, D., Nezu, J., Kawahara, E. and Tsuji, A. (2001) Na(+)-coupled transport of L-carnitine *via* high-affinity carnitine transporter OCTN2 and its subcellular localization in kidney. Biochim. Biophys. Acta 1512, 273–284.
6 Tamai, I., Ohashi, R., Nezu, J., Yabuuchi, H., Oku, A., Shimane, M., Sai, Y. and Tsuji, A. (1998) Molecular and functional identification of sodium ion-dependent, high affinity human carnitine transporter OCTN2. J. Biol. Chem. 273, 20378–20382.
7 Wu, X., Huang, W., Prasad, P. D., Seth, P., Rajan, D. P., Leibach, F. H., Chen, J., Conway, S. J. and Ganapathy, V. (1999) Functional characteristics and tissue distribution pattern of organic cation transporter 2 (OCTN2), an organic cation/carnitine transporter. J. Pharmacol. Exp. Ther. 290, 1482–1492.
8 Wu, X., Prasad, P. D., Leibach, F. H. and Ganapathy, V. (1998) cDNA sequence, transport function, and genomic organization of human OCTN2, a new member of the organic cation transporter family. Biochem. Biophys. Res. Commun. 246, 589–595.
9 Scholte, H. R., Rodrigues Pereira, R., de Jonge, P. C., Luyt-Houwen, I. E., Hedwig, M., Verduin, M. and Ross, J. D. (1990) Primary carnitine deficiency. J. Clin. Chem. Clin. Biochem. 28, 351–357.
10 Burwinkel, B., Kreuder, J., Schweitzer, S., Vorgerd, M., Gempel, K., Gerbitz, K. D. and Kilimann, M. W. (1999) Carnitine transporter OCTN2 mutations in systemic primary carnitine deficiency: A novel Arg169Gln mutation and a recurrent Arg282ter mutation associated with an unconventional splicing abnormality. Biochem. Biophys. Res. Commun. 261, 484–487.
11 Mayatepek, E., Nezu, J., Tamai, I., Oku, A., Katsura, M., Shimane, M. and Tsuji, A. (2000) Two novel missense mutations of the OCTN2 gene (W283R and V446F) in a patient with primary systemic carnitine deficiency. Hum. Mutat. 15, 118.
12 Nezu, J., Tamai, I., Oku, A., Ohashi, R., Yabuuchi, H., Hashimoto, N., Nikaido, H., Sai, Y., Koizumi, A., Shoji, Y., Takada, G., Matsuishi, T., Yoshino, M., Kato, H., Ohura, T., Tsujimoto, G., Hayakawa, J., Shimane, M. and Tsuji, A. (1999) Primary systemic carnitine deficiency is caused by mutations in a gene encoding sodium ion-dependent carnitine transporter. Nat. Genet. 21, 91–94.
13 Rahbeeni, Z., Vaz, F. M., Al-Hussein, K., Bucknall, M. P., Ruiter, J., Wanders, R. J. and Rashed, M. S. (2002) Identification of two novel mutations in OCTN2 from two Saudi patients with systemic carnitine deficiency. J. Inherit. Metab. Dis. 25, 363–369.
14 Tang, N. L., Ganapathy, V., Wu, X., Hui, J., Seth, P., Yuen, P. M., Wanders, R. J., Fok, T. F. and Hjelm, N. M. (1999) Mutations of OCTN2, an organic cation/carnitine transporter, lead to deficient cellular carnitine uptake in primary carnitine deficiency. Hum. Mol. Genet. 8, 655–660.
15 Vaz, F. M., Scholte, H. R., Ruiter, J., Hussaarts-Odijk, L. M., Pereira, R. R., Schweitzer, S., de Klerk, J. B., Waterham, H. R. and Wanders, R. J. (1999) Identification of two novel mutations in OCTN2 of three patients with systemic carnitine deficiency. Hum. Genet. 105, 157–161.
16 Lamhonwah, A. M. and Tein, I. (1998) Carnitine uptake defect: Frameshift mutations in the human plasmalemmal carnitine transporter gene. Biochem. Biophys. Res. Commun. 252, 396–401.
17 Wang, Y., Ye, J., Ganapathy, V. and Longo, N. (1999) Mutations in the organic cation/carnitine transporter OCTN2 in primary carnitine deficiency. Proc. Natl. Acad. Sci. USA 96, 2356–2360.
18 Makhseed, N., Vallance, H. D., Potter, M., Waters, P. J., Wong, L. T., Lillquist, Y., Pasquali, M., Amat di San Filippo, C. and Longo, N. (2004) Carnitine transporter defect due to a novel mutation in the SLC22A5 gene presenting with peripheral neuropathy. J. Inherit. Metab. Dis. 27, 778–780.
19 Rijlaarsdam, R. S., van Spronsen, F. J., Bink-Boelkens, M. T., Reijngoud, D. J., Wanders, R. J., Niezen-Koning, K. E., Van der Sluijs, F. H., Dorland, B. and Beaufort-Krol, G. C. (2004) Ventricular fibrillation without overt cardiomyopathy as first presentation of organic cation transporter 2-deficiency in adolescence. Pacing Clin. Electrophysiol. 27, 675–676.
20 Famularo, G., De Simone, C., Trinchieri, V. and Mosca, L. (2004) Carnitines and its congeners: A metabolic pathway to the regulation of immune response and inflammation. Ann. N. Y. Acad. Sci. 1033, 132–138.
21 Ferrari, R., Merli, E., Cicchitelli, G., Mele, D., Fucili, A. and Ceconi, C. (2004) Therapeutic effects of L-carnitine and propionyl-L-carnitine on cardiovascular diseases: A review. Ann. N. Y. Acad. Sci. 1033, 79–91.
22 Ng, C. M., Blackman, M. R., Wang, C. and Swerdloff, R. S. (2004) The role of carnitine in the male reproductive system. Ann. N. Y. Acad. Sci. 1033, 177–188.
23 Ohtani, Y., Endo, F. and Matsuda, I. (1982) Carnitine deficiency and hyperammonemia associated with valproic acid therapy. J. Pediatr. 101, 782–785.
24 Kuntzer, T., Reichmann, H., Bogousslavsky, J. and Regli, F. (1990) Emetine-induced myopathy and carnitine deficiency. J. Neurol. 237, 495–496.
25 Holme, E., Greter, J., Jacobson, C. E., Lindstedt, S., Nordin, I., Kristiansson, B. and Jodal, U. (1989) Carnitine deficiency induced by pivampicillin and pivmecillinam therapy. Lancet 2, 469–473.
26 Ohashi, R., Tamai, I., Yabuuchi, H., Nezu, J. I., Oku, A., Sai, Y., Shimane, M. and Tsuji, A. (1999) Na(+)-dependent carnitine transport by organic cation transporter (OCTN2): Its pharmacological and toxicological relevance. J. Pharmacol. Exp. Ther. 291, 778–784.
27 Ganapathy, M. E., Huang, W., Rajan, D. P., Carter, A. L., Sugawara, M., Iseki, K., Leibach, F. H. and Ganapathy, V. (2000) Beta-lactam antibiotics as substrates for OCTN2, an organic cation/carnitine transporter. J. Biol. Chem. 275, 1699–1707.
28 Spaniol, M., Brooks, H., Auer, L., Zimmermann, A., Solioz, M., Stieger, B. and Krahenbuhl, S. (2001) Development and characterization of an animal model of carnitine deficiency. Eur. J. Biochem. 268, 1876–1887.
29 Stieger, B., Hagenbuch, B., Landmann, L., Hochli, M., Schroeder, A. and Meier, P. J. (1994) In situ localization of the hepatocytic Na^+/taurocholate cotransporting polypeptide in rat liver. Gastroenterology 107, 1781–1787.
30 Salmon, P., Oberholzer, J., Occhiodoro, T., Morel, P., Lou, J. and Trono, D. (2000) Reversible immortalization of human primary cells by lentivector-mediated transfer of specific genes. Mol. Ther. 2, 404–414.
31 Allen, F. H. and Motherwell, W. D. (2002) Applications of the Cambridge Structural Database in organic chemistry and crystal chemistry. Acta Crystallogr. B 58, 407–422.
32 O'Neil, M. J. (2006) The Merck Index: An Encyclopedia of Chemicals, Drugs and Biologicals. John Wiley & Sons, New York.
33 Brass, E. P. and Hoppel, C. L. (1978) Carnitine metabolism in the fasting rat. J. Biol. Chem. 253, 2688–2693.
34 Wagner, C. A., Lukewille, U., Kaltenbach, S., Moschen, I., Broer, A., Risler, T., Broer, S. and Lang, F. (2000) Functional and pharmacological characterization of human Na(+)-carnitine cotransporter hOCTN2. Am. J. Physiol. Renal Physiol. 279, F584–591.
35 Sekine, T., Kusuhara, H., Utsunomiya-Tate, N., Tsuda, M., Sugiyama, Y., Kanai, Y. and Endou, H. (1998) Molecular cloning and characterization of high-affinity carnitine transporter from rat intestine. Biochem. Biophys. Res. Commun. 251, 586–591.

36 Georges, B., Galland, S., Rigault, C., Le Borgne, F. and Demarquoy, J. (2003) Beneficial effects of L-carnitine in myoblastic C2C12 cells. Interaction with zidovudine. Biochem. Pharmacol. 65, 1483–1488.
37 Kido, Y., Tamai, I., Ohnari, A., Sai, Y., Kagami, T., Nezu, J., Nikaido, H., Hashimoto, N., Asano, M. and Tsuji, A. (2001) Functional relevance of carnitine transporter OCTN2 to brain distribution of L-carnitine and acetyl-L-carnitine across the blood-brain barrier. J. Neurochem. 79, 959–969.
38 Berman, H. M., Westbrook, J., Feng, Z., Gilliland, G., Bhat, T. N., Weissig, H., Shindyalov, I. N. and Bourne, P. E. (2000) The Protein Data Bank. Nucleic Acids Res. 28, 235–242.
39 Rigault, C., Dias, J. V., Demarquoy, J. and Le Borgne, F. (2008) Characteristics of L-carnitine import into heart cells. Biochimie 90, 542–546.